EFFECT OF COMPRESSIBILITY ON THE VELOCITY GRADIENT TENSOR AT FREE SHEAR FLOW BOUNDARIES

Joseph Mathew
Department of Aerospace Engineering
Indian Institute of Science
Bangalore 560012 INDIA
email: joseph@aero.iisc.ernet.in

S. Ghosh
Lehrstuhl fuer Aerodynamik
Technische Universitaet Muenchen
Boltzmannstr. 15, D-85748 Garching, GERMANY
email: Somnath.Ghosh@aer.mw.tum.de

ABSTRACT

Analyses of the invariants of the velocity gradient tensor were performed on flow fields obtained by DNS of compressible plane mixing layers at convective Mach numbers $M_c = 0.15$ and 1.1. Joint pdfs of the 2nd and 3rd invariants were examined at turbulent/nonturbulent (T/NT) boundaries—defined as surfaces where the local vorticity first exceeds a threshold fraction of the maximum of the mean vorticity. By increasing the threshold from very small levels, the boundary points were moved closer into the turbulent region, and the effects on the pdfs of the invariants were observed. Generally, T/NT boundaries are in sheet-like regions at both Mach numbers. At the higher Mach number a distinct lobe appears in the joint pdf isolines which has not been observed/reported before. A connection to the delayed entrainment and reduced growth rate of the higher Mach number flow is proposed.

INTRODUCTION

Turbulence studies may be divided into those based on its stochastic nature and those searching for orderly behavior. Coherent structures such as spanwise rollers in plane mixing layers and hairpins near walls are examples of such order. Processes in turbulent flows may then be understood in terms of the dynamics of these structures, and their effects on surrounding flow. Analyses of the velocity gradient tensor in turbulent flow fields reveal the local flow topology and motivate a mechanistic view of the processes that fluid packets undergo. The present study is directed towards further understanding of turbulent entrainment in free shear flows following from two main results: First, the recent finding that the entrainment *process* occurs close to the boundary between turbulent and nonturbulent regions (Mathew & Basu, 2002), and second, which is more widely known, that compressibility has a stabilizing effect on free shear flows (see, for example, Sarkar, 1995), thereby significantly reducing its growth rate. Our previous study of the effects of compressibility (and heat release) on entrainment (Mathew *et al.*, 2008) revealed that the process gets delayed, even though it still occurs near the boundaries of the turbulent region, as in incompressible flows. To understand the process better, we have examined some properties of the velocity gradient tensor near the boundaries of turbulent, plane mixing layers at different compressibility levels, using DNS flow fields.

Chong *et al.* (1990) classified the local structure of velocity fields in terms of the three invariants, labelled P, Q and R, of the velocity gradient tensor (VGT). In different parts of the P-Q-R space, the local streamlines depict foci (streamlines circling to or away from an axis) with either stretching or compressing, nodes and saddles. Soria *et al.* (1994) examined the joint distributions of Q and R for $P = 0$ (incompressible flow) in a turbulent mixing layer. Most of the distribution occupied a teardrop-shaped region of the Q-R plane. Ooi *et al.* (1999) found that successive positions of a fluid packet correspond to a trajectory that circles the origin of the Q-R graph. Thus fluid packets occupy successively, sheet-like regions, then regions with stretching followed by compression in a repetitive cycle. Flow fields were from DNS of incompressible, homogeneous isotropic turbulence.

Two previous studies are more closely related to the present work. Suman & Girimaji (2010) examined the modifications due to compressibility in a DNS of decaying, homogeneous, isotropic turbulence. They found changes to the shape of the isolines of the Q-R distribution in regions where the dilatation was significant. At high levels of dilatation, the distribution occupies a smaller part of the Q-R plane, close to the cusp of the discriminant curve. We find, however, a different change due to compressibility in that the footprint of the distribution extends into a different quadrant. Such a change to the teardrop region has never been observed before. Da Silva & Pereira (2008) performed VGT analyses at locations near the

turbulent/nonturbulent (T/NT) interface of an incompressible, plane jet. They observed transition to states representative of fully turbulent regions to occur over a short distance. They examined invariants of the strain-rate and rotation-rate tensors also, and noted the change from a strain-rate dominance just outside the turbulent region to an equipartitioned state within. Here, we have examined distributions of these invariants near turbulence boundaries of *compressible* plane mixing layers. The data and observations are particularly valuable because the mixing layers are at Reynolds numbers well above 10000 (based on vorticity thickness), which is above the mixing transition level.

DEFINITIONS AND FLOW FIELDS

The velocity gradient tensor $\mathbf{A}$, whose elements are $A_{ij} = \partial u_i/\partial x_j$, has three invariants: $P = -\text{trace}\mathbf{A}$; $Q = \frac{1}{2}\left[P^2 - \text{trace}(\mathbf{A^2})\right]$; $R = -\det(\mathbf{A})$. For incompressible flow $P = 0$. Real values of the eigenvalues of $\mathbf{A}$ are bounded by a surface on which the discriminant $D = 27R^2 + (4P^3 - 18PQ)R + (4Q^3 - P^2Q^2) = 0$. $\mathbf{A}$ can be split into a symmetric strain-rate and skew-symmetric, rotation-rate parts: $\mathbf{A} = \mathbf{S} + \mathbf{W}$. With subscripts S and W to denote invariants of these two tensors, $P_W = R_W = 0$ for all flows; $P_S = P$, $Q_S = -(1/2)S_{ij}S_{ji}$, $R_S = -(1/3)S_{ij}S_{jk}S_{ki}$ and $Q_W = -(1/2)W_{ij}W_{ji}$. The elements of $\mathbf{W}$ are one-half of vorticity components. So $Q_W \geq 0$ and is proportional to the enstrophy, while $Q_S \leq 0$ and is proportional to the viscous dissipation for incompressible flow ($\varepsilon = 2\nu S^2 = -4\nu Q_S$). For compressible flow, $Q_S = (1/2)(P^2 - S_{ij}S_{ji})$. If enstrophy dominates dissipation the region is likely to be tube-like; a region of rigid body rotation has vorticity but no dissipation.

The flow fields are from temporal DNS of compressible, plane mixing layers obtained by Mahle (2007) (also described in Mathew *et al.*, 2008). The extent of compressibility is measured by the convective Mach number $M_c = \Delta u/(c_1 + c_2)$, where Δu is the velocity difference between the two streams where sonic speeds are c_1 and c_2. Three cases with $M_c = 0.15$, 0.7 and 1.1 obtained on a grid of 768 streamwise, 192 spanwise and 576 cross-layer points were available. Flow fields were at times when the mixing layer undergoes a self-similar evolution.

ANALYSES AND RESULTS

Estimates of the joint pdf of invariants (Q, R), (Q_S, R_S), and (Q_S, Q_W) were obtained and plotted by dividing the three standard deviation range of each random variable into 200 equi-spaced bins. In the following figures iso-pdf curves of these pairs of variables are shown. The VGT was scaled with the maximum of the mean vorticity of the flow field at the selected instant.

We consider pdfs of 1) all gridpoints in the simulation field, 2) points in the turbulent and non-turbulent regions separately, and 3) points which are at the boundary between these two regions. Issues in defining the turbulent region are discussed in Mathew & Basu (2002) as well as in other references cited therein. We use the term boundary rather than interface because the latter denotes a thin region between turbulent and nonturbulent regions. Here, the boundary of the turbulent region is located at gridpoints where the vorticity magnitude first exceeds a threshold level. The threshold is a fraction of the maximum of the mean vorticity in the flow field at that time. The threshold may be taken as, say, 10%, but the effect of varying this level is also considered below.

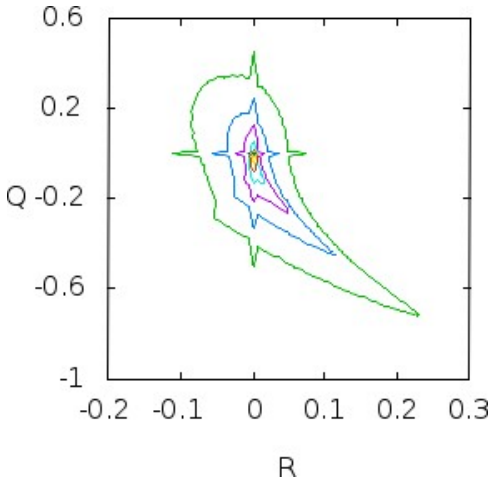

Figure 1. Iso-lines of joint pdf of Q and R over all gridpoints at $M_c = 0.15$.

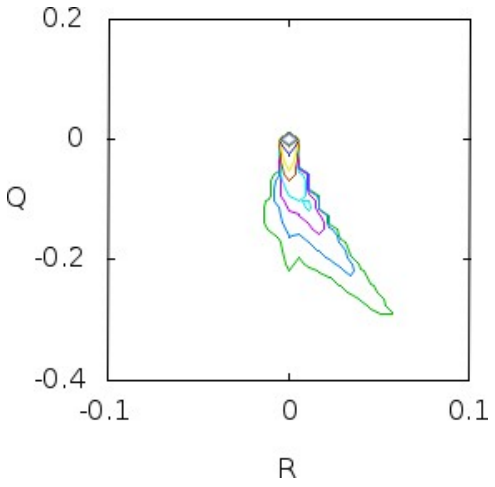

Figure 2. Joint pdf from gridpoints in the nonturbulent region at $M_c = 0.15$.

Q – R distributions

All figures show isolines of the joint pdf of Q-R or Q_s-R_s. Contours are nested curves at levels 0.00001, 0.00003, 0.0001, 0.0003, 0.001, 0.003, 0.01, 0.03, 0.1, 0.3 beginning from the outermost. Figure 1 is the joint pdf over the whole field for the essentially incompressible flow ($M_c = 0.15$). The shape of the isolines is very similar to those obtained in the several previous studies in different flows (Ooi *et al.*, 1999; Da Silva & Pereira, 2008; Suman & Girimaji, 2010). At higher M_c, the shape is the same but the range of Q and R fall slightly. The same shapes are obtained when the turbulent region alone is considered also. The long tail in the region $Q < 0$, $R > 0$ implies a vortex-sheet-like region with two ex-

tensional and one compressive straining directions. The head, $Q > 0$ implies a local topology that is vortex-tube-like with stretching where $R < 0$ and compressing where $R > 0$.

Figure 2 is of the nonturbulent region alone at $M_c = 0.15$. These are from locations where the vorticity is less than 10% of the maximum mean vorticity. The lobe to the lower right ($Q < 0$, $R > 0$) implies that the flow is sheet-like. We can deduce from these two figures that during the initial stages of entrainment, fluid packets travel into turbulent regions which are sheet-like. Indeed, an analysis using the round-jet simulation of Mathew & Basu (2002), showed that particle pathlines beginning in the surrounding irrotational region begin near the origin in the *Q*-*R* plane, move along the 4th-quadrant lobe, reverse direction to travel towards the 2nd quadrant and then to the 1st quadrant. There is support for this view in the analyses of Da Silva & Pereira (2008) who have presented *Q*-*R* plots for different locations across the turbulent/nonturbulent interface from their simulations of an incompressible plane jet. This progression through different quadrants corresponds to fluid particles entering a sheet-like region initially, moving to a region of a stretching vortex tube, and then a compressing vortex tube. We may speculate that fluid particles enter in the sheet-like region between vortices at the turbulent-nonturbulent interface and acquire vorticity (become entrained); this sheet then rolls up and undergoes stretching and is then a part of the common dynamics of the interior of the turbulent flow described in Ooi *et al.* (1999).

The shapes of the distributions are similar at the intermediate Mach number $M_c = 0.7$. At $M_c = 1.1$, some qualitative differences begin to appear. Figure 3(*a*) shows isolines of the joint distribution for locations in the nonturbulent region using all such points in the simulation. When a *subset* of the simulation region is taken, a new lobe in the distribution appears in the 3rd quadrant (Figure 3(*b*)). Here, a quarter of the streamwise extent has been taken. This 3rd-quadrant lobe is a less frequent topology and is not evident when the full domain is considered. Such a lobe does not appear when a partial domain is taken at the lower Mach number; then, distributions for every subdomain resembles that of the full domain. Moreover, this has never been observed before because the analyses have been of incompressible flow, or of compressible flow in turbulent regions only.

Q − R distributions at T/NT boundary Figure 2 was obtained by taking the nonturbulent region to lie outside the mixing layer wherever the vorticity magnitude was below the 10% threshold. Changing this threshold changes the location of the boundary and can show different stages in the entrainment process because this process occurs within a short distance of this boundary. At higher threshold levels the boundary moves progressively into the turbulent region. In Figure 4 *Q*-*R* distributions for locations at this boundary are shown for different threshold levels from the $M_c = 0.15$ mixing layer. At the 1% threshold level, (Fig 2(*a*) most places on the T/NT boundary have Q and R in the 4th quadrant, in sheet-like flows. At 10%, the boundary is closer to the fully turbulent region; most regions are still sheet-like though tube-like regions (3rd quadrant) are also present (Fig 2(*b*). There is little change on increasing the threshold to 15%.

Figure 5 shows distributions on T/NT boundary at the higher Mach number. Now, at 1%, 10%, and 15% threshold levels the 3rd-quadrant lobe that was observed in Figure 3(*b*) is quite clear. Here, the full simulation has been used—not just the quarter of the field considered for Figure 3(*b*).

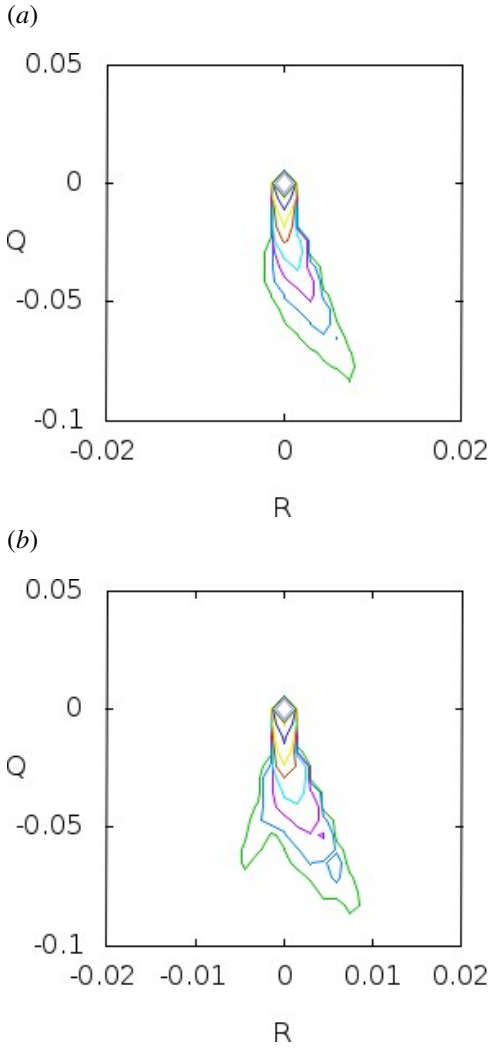

Figure 3. Joint pdf of *Q*-*R* for $M_c = 1.1$ in nonturbulent region. (*a*) full simulation domain; (*b*) a quarter of streamwise extent only

$Q_S - R_S$ distributions

A similar analysis of the invariants of the strain rate tensor $\mathbf{S}$ confirms the effect due to compressibility at the T/NT boundary. At $M_c = 0.15$ most of the boundary points are in regions with two extensional and one compressive strain rates (4th quadrant in Q_s-R_s plane; Fig. 6). Far less frequently there are regions with extension in one direction and compression in the other two (3rd quadrant). The shape of the distribution remains similar at different thresholds but strain rates increase as the boundary moves into the turbulent region. At $M_c = 1.1$ also, generally, the local structure of the strain-rate field is similar as is evident in Figures 7(*a*) and (*b*) where threshold levels are 1% and 10%, respectively. Figures 7(*c*) was obtained by taking only a quarter of the streamwise extent and

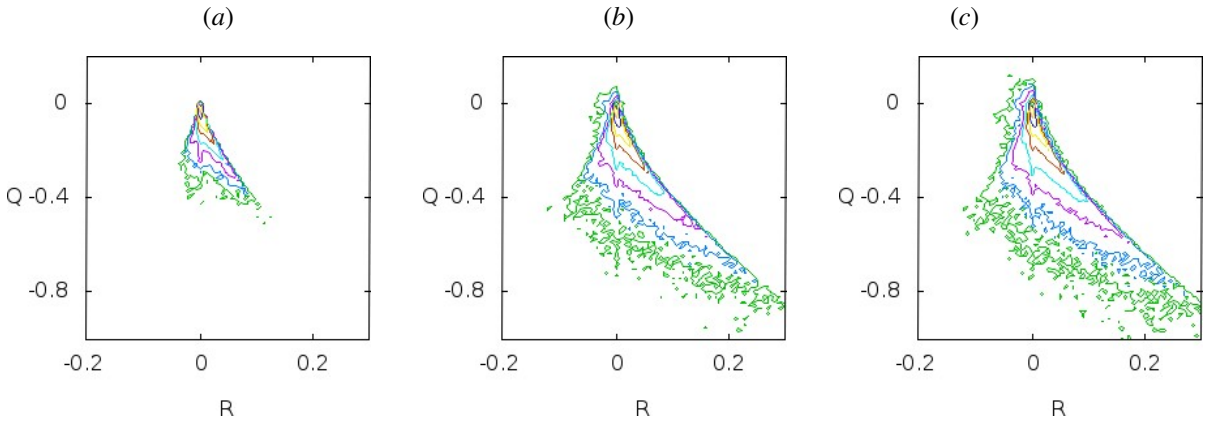

Figure 4. Joint pdf of Q-R for $M_c = 0.15$ along T/NT boundary taken as iso-surfaces where vorticity magnitude crosses a threshold level. (a) 1% (b) 10% (c) 15%.

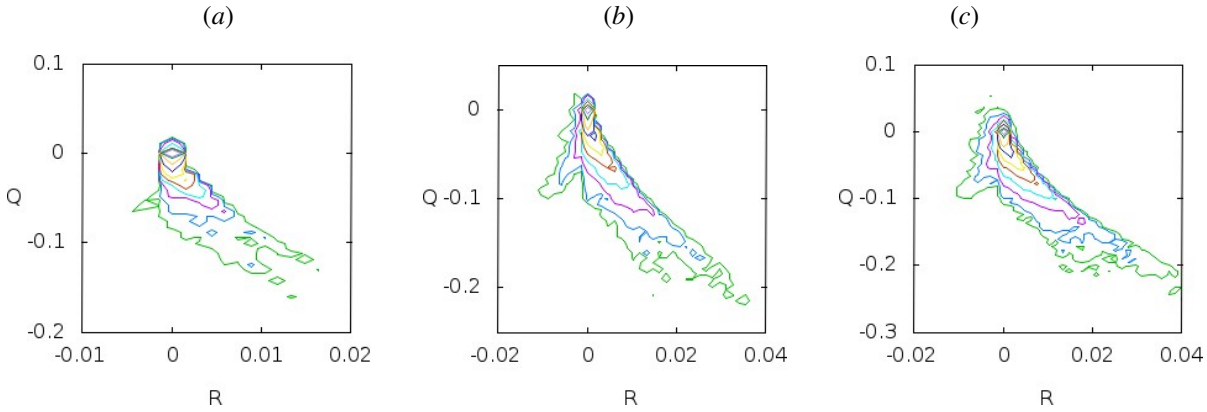

Figure 5. Joint pdf of Q-R for $M_c = 1.1$ along T/NT boundary. Threshold levels are (a) 1% (b) 10% (c) 15%.

with threshold level set to 10%. Again a distinct lobe into the 3rd quadrant appears indicating a distinct tube-like flow over some parts of the T/NT boundary as a compressibility effect.

DISCUSSION AND CONCLUSIONS

In this study, invariants of the velocity gradient tensor and its symmetric part were computed from fields obtained from DNS of compressible plane mixing layers. One simulation at the convective Mach number of 0.15 is of an essentially incompressible flow whereas the second at 1.1 exhibits significant compressibility effects. The Reynolds numbers based on velocity differences and vorticity thickness are well above 10,000, which is above the mixing transition level. So the results should not have any low Reynolds number limitations.

The structure of the flow was examined by plotting isolines of joint pdfs of the 2nd and 3rd invariants Q and R, or Q_s and R_s. In both cases the overall ranges of the distribution of the invariants (shapes of joint pdf isolines) are as has been observed before for incompressible fields of homogeneous turbulence (Ooi *et al.*, 1999) and plane jets (Da Silva & Pereira, 2008), and compressible, homogeneous turbulence (Suman & Girimaji, 2010). Results for the particular focus of this study—properties of the turbulent/nonturbulent interface—also agree with the findings of (Da Silva & Pereira, 2008) who took an incompressible plane jet. As the boundary is defined more conservatively into the turbulent region, most parts of the boundary have Q-R values in the 4th quadrant, close to the discriminant $D > 0$ curve. This indicates regions of sheet-like flow. The dominance of isolines in the 4th quadrant of the Q_s-R_s diagram also indicates regions with stretching in two perpendicular directions as in sheets, or an interior stagnation point flow. These are flows that can develop between counter-rotating or co-rotating vortices, respectively.

The notable difference due to compressibility is the appearance of a distinct lobe into the 3rd quadrant in the isolines of the distributions of both Q-R and Q_s-R_s joint pdfs. This lobe is not always evident when the full simulation field is considered. For example, when all points in the nonturbulent region are considered, the lobe was clear only when a subset of the field—a quarter of the streamwise extent—was taken for analyses; otherwise it is suppressed by the more frequent contributions from other topolgy. Nevertheles, it is clearly seen when points at the T/NT boundary alone are taken over the full simulation domain. The third quadrant in the Q-R or Q_s-R_s plane implies a tube-like structure. We may infer that

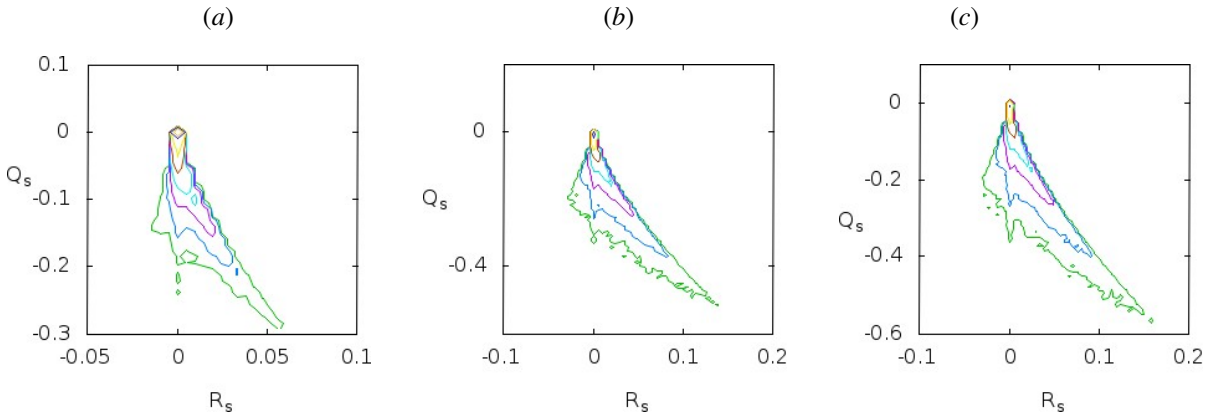

Figure 6. Joint pdf of Q_s-R_s for $M_c = 0.15$ along T/NT boundary. Threshold levels are (*a*) 1% (*b*) 10% (*c*) 15%.

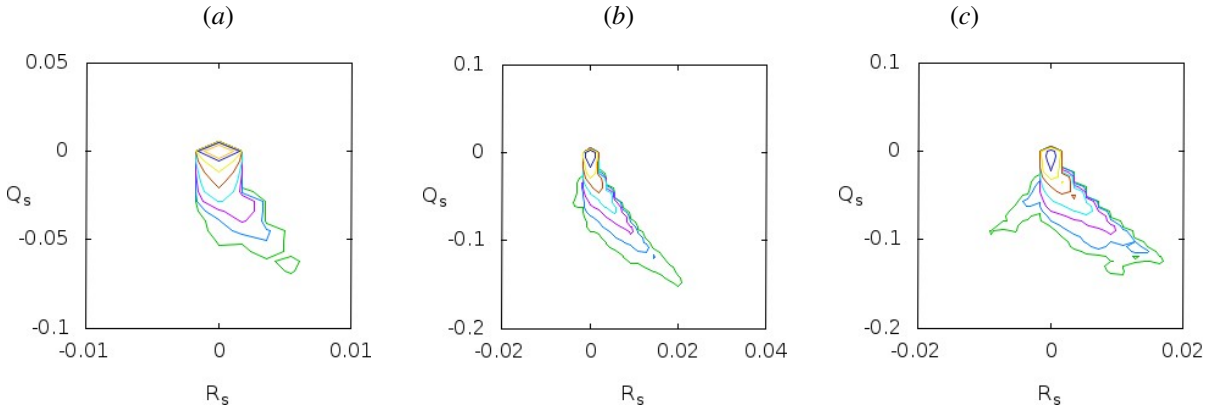

Figure 7. Joint pdf of Q_s-R_s for $M_c = 1.1$ along T/NT boundary. Threshold levels are (*a*) 1% (*b*) 15% (*c*) 15%; quarter of simulation domain taken.

this lobe is a signature of the changes to the entrainment process. In previous studies using fluid particle tracking, Mathew *et al.* (2008) observed that the entrainment process of compressible mixing layers is similar to that in incompressible flow in that it still takes place at the T/NT interface but gets significantly delayed as compressibility (or heat release) levels increase. We anticipate that the *distinct* 3rd quadrant lobe found at the higher Mach number is a manifestation of the delayed entrainment. When there is such a delay, fluid particles undergo *irrotational* circular, possibly spiralling, motions induced by the nearby vortices. Such spiralling pathlines in the irrotational region surrounding a round jet can be seen in Mathew & Basu (2002). Here, a confirmation is beyond the scope of the present study because only flow fields at some instants were available for the analyses. It would be necessary to follow the evolution of fluid packets during the simulations to clear understanding.

Finally, Fig. 8 shows Q-R and Q_s-R_s distributions at both Mach numbers well within the turbulent region. It suffices to take the threshold level as a large fraction; here it is 0.5. It is intriguing that the distributions look remarkably similar at the two Mach numbers. Perhaps the effect of compressibility in the interior of the turbulent region on the velocity gradient tensor and the implied local topology is not a qualitative difference. There are quantative differences: the range of values taken by the invariants are certainly smaller at the higher Mach number. The qualitative difference at the T/NT boundary at significant compressibility levels may arise from differences in processes at the T/NT interface. Of course, there may not be a cause-effect mechanism—just differences in structure and process that are consistent with the enhanced compressibility possible in the flow.

Acknowledgments

J. M. is grateful to the Erasmus Mundus WILLPower program which supported his visit to Technische Universitaet Muenchen where the initial analyses were done. He also thanks Prof. R. Friedrich for useful discussions of this study, and for graciously hosting the visit.

REFERENCES

Chong, M. S., Perry, A. E. & Cantwell, B. J. 1990 A general classification of three-dimensional flow fields. *Phys. Fluids A* **2 (5)**, 765–777.

Da Silva, C. B. & Pereira, J. C. F. 2008 Invariants of the velocity-gradient, rate-of-strain, and rate-of-rotation ten-

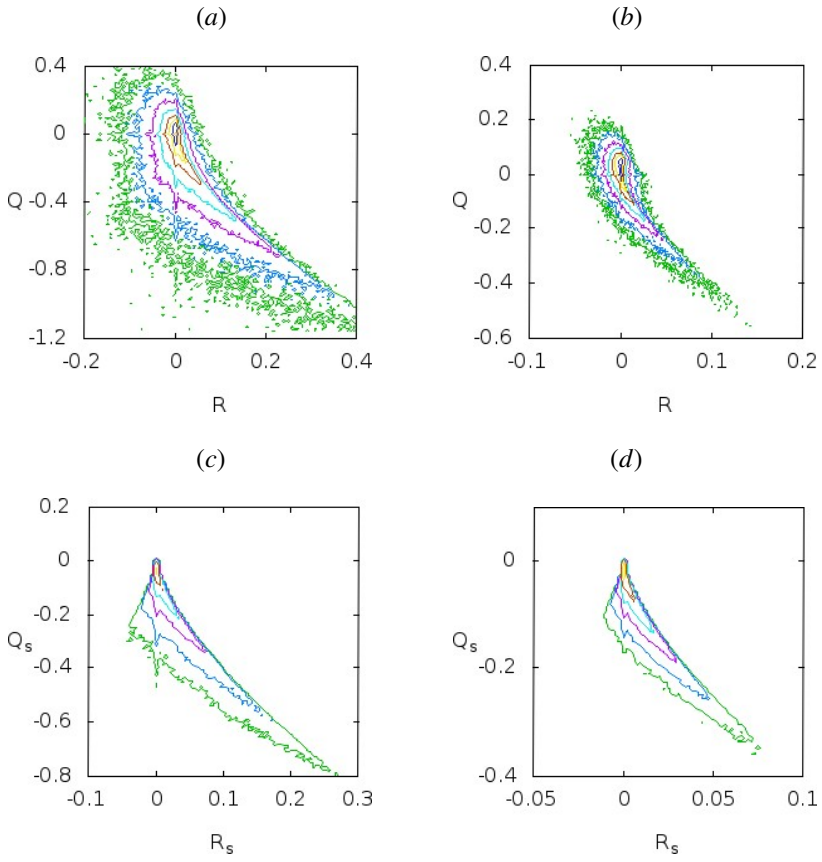

Figure 8. Joint pdfs of Q-R and Q_s-R_s on isosurface within turbulent region (50% threshold). (a, c): $M_c = 0.15$; (b, d): $M_c = 1.1$.

sors across the turbulent/nonturbulent interface in jets. *Phys. Fluids* **20**, 055101.

Mahle, I. 2007 Direct and large-eddy simulation of inert and reacting compressible turbulent shear layers. PhD thesis, Technische Universitaet Muenchen, Munich.

Mathew, J & Basu, AJ 2002 Some characteristics of entrainment at a cylindrical turbulence boundary. *Phys. Fluids* **14** (7), 2065–2072.

Mathew, Joseph, Mahle, Inga & Friedrich, Rainer 2008 Effects of compressibility and heat release on entrainment processes in mixing layers. *J. Turbulence* **9** (14), 1–12.

Ooi, A., Martin, J., Soria, J. & Chong, M. S. 1999 A study of the evolution and characteristics of the invariants of the velocity-gradient tensor in isotropic turbulence. *J. Fluid Mech.* **381**, 141–174.

Sarkar, S. 1995 The stabilizing effect of compressibility in turbulent shear flow. *J. Fluid Mech.* **282**, 163 – 186.

Soria, J., Sondergaard, R., Cantwell, B. J., Chong, M. S. & Perry, A. E. 1994 A study of the fine scale motions of incompressible time-developing mixing layers. *Phys. Fluids* **6** (2), 871–884.

Suman, S. & Girimaji, S. S. 2010 Velocity gradient invariants and local flow-field topology in compressibile turbulence. *J. Turbulence* **11** (2), 1–24.